Activin A Promotes Regulatory T-cell–Mediated Immunosuppression in Irradiated Breast Cancer

Mara De Martino[1], Camille Daviaud[1], Julie M. Diamond[1,2,3], Jeffrey Kraynak[1], Amandine Alard[4], Silvia C. Formenti[1,5], Lance D. Miller[6,7], Sandra Demaria[1,5,8], and Claire Vanpouille-Box[1,5]

ABSTRACT

Increased regulatory T cells (Treg) after radiotherapy have been reported, but the mechanisms of their induction remain incompletely understood. TGFβ is known to foster Treg differentiation within tumors and is activated following radiotherapy. Thus, we hypothesized that TGFβ blockade would result in decreased Tregs within the irradiated tumor microenvironment. We found increased Tregs in the tumors of mice treated with focal radiotherapy and TGFβ blockade. This increase was mediated by upregulation of another TGFβ family member, activin A. *In vitro*, activin A secretion was increased following irradiation of mouse and human breast cancer cells, and its expression was further enhanced upon TGFβ blockade. *In vivo*, dual blockade of activin A and TGFβ was required to decrease intratumoral Tregs in the context of radiotherapy. This resulted in an increase in $CD8^+$ T-cell priming and was associated with a reduced tumor recurrence rate. Combination of immune checkpoint inhibitors with the dual blockade of activin A and TGFβ led to the development of tumor-specific memory responses in irradiated breast cancer. Supporting the translational value of activin A targeting to reduce Treg-mediated immunosuppression, retrospective analysis of a public dataset of patients with breast cancer revealed a positive correlation between activin A gene expression and Treg abundance. Overall, these results shed light on an immune escape mechanism driven by activin A and suggest that dual targeting of activin A and TGFβ may be required to optimally unleash radiation-induced antitumor immunity against breast cancer.

Introduction

Identifying treatments that can generate tumor-specific T-cell responses is an area of active investigation in immunotherapy (1). Tumor-targeted radiotherapy (RT) has shown the ability to foster antitumor immunity (2), but its positive effects are mitigated by immune-inhibitory mechanisms that preexist or are exacerbated by RT (3). Among them, an increase in regulatory $CD4^+$ T cells (Treg) has been observed following focal tumor RT in mice as well as patients (4, 5).

The mechanisms of increased radiation-induced Tregs remain elusive. TGFβ is a pleiotropic cytokine produced by the majority of immune cells and is critical in the differentiation of naïve $CD4^+$ T cells into $CD4^+FoxP3^+$ Tregs (6, 7). *Bona fide* TGFβ is sequestrated into the tumor microenvironment (TME) in the inactive form, where its bioavailability is both regulated by its secretion and by extracellular mechanisms that can activate it, like reactive oxygen species (ROS) generated by RT. ROS modify the backbone of the latency-associated peptide–TGFβ complex to release the active growth factor (8, 9). Consequently, radiation-induced increases in active TGFβ could be responsible, at least in part, for the observed increase in Tregs subsequent to RT. However, inhibition of TGFβ has failed to reduce Tregs in an irradiated melanoma tumor model, challenging the role of TGFβ in Treg expansion after RT (10).

Activin A belongs to the TGFβ superfamily and shares the canonical SMAD2/3 pathway with TGFβ (11, 12). However, activin A signals through its own set of receptors that include activin A type II (ActRIIA, ACtRIIB) and type I receptors (mainly ActRIB, but also ActRIA and ActRIC; aka ALK4, ALK2, and ALK7, respectively; ref. 11). Consequently, activin A and TGFβ exhibit overlapping functions including, but not limited to, the induction of FoxP3 expression and the generation of Tregs (13, 14). Of note, activin A is found to compensate for the lack of SMAD2/3 phosphorylation when TGFβ signaling is impaired in the context of vascular development, where knockdown of the TGFβ type-I receptor (aka ALK5, TGFBR1) in the embryonic day 9.5 (E9.5) of development results in the upregulation of the activin A/ALK4 pathway (15), thus suggesting a cross-talk between these cytokines to presumably maintain homeostasis and basic cellular functions.

Activin A expression is elevated in multiple cancers (16–18) and is also induced in response to RT, as demonstrated in lung and pancreatic carcinoma cells (19).

The emerging role in carcinogenesis of activin A, its link with TGFβ, and its described ability to promote Treg-mediated immunosuppression in allergic disorders (13, 14, 20) led us to investigate the role of activin A in the radiation-induced increase in Tregs. Here, we demonstrated that tumor-derived activin A was responsible for relapses of murine mammary carcinomas in the context of RT and antibody-mediated TGFβ blockade. Using two mouse mammary carcinomas models with different baseline expression of activin A, 4T1 (high activin A–secreting cells), and TSA (low activin A–secreting cells), we showed that the increase of Tregs in irradiated tumors depended on

[1]Department of Radiation Oncology, Weill Cornell Medicine, New York, New York. [2]Department of Pathology, New York University School of Medicine, New York, New York. [3]Endless Frontier Labs, New York, New York. [4]Cancer Research Center of Toulouse (CRCT), INSERM UMR 1037-University Toulouse III Paul Sabatier, Toulouse, France. [5]Sandra and Edward Meyer Cancer Center, New York, New York. [6]Wake Forest Baptist Comprehensive Cancer Center, Winston-Salem, North Carolina. [7]Department of Cancer Biology, Wake Forest School of Medicine, Winston-Salem, North Carolina. [8]Department of Pathology and Laboratory Medicine, Weill Cornell Medicine, New York, New York.

Note: Supplementary data for this article are available at Cancer Immunology Research Online (http://cancerimmunolres.aacrjournals.org/).

M. De Martino and C. Daviaud contributed equally to this article.

Corresponding Author: Claire Vanpouille-Box, Weill Cornell Medicine, 1300 York Avenue, Room E215A, Box 169, New York, NY 10065. Phone: 646-962-2125; Fax: 212-746-7815; E-mail: clv2002@med.cornell.edu

Cancer Immunol Res 2021;9:89–102

doi: 10.1158/2326-6066.CIR-19-0305

both TGFβ and activin A. Treg increase regulated $CD8^+$ T-cell priming, tumor relapse, and survival of the mice. The addition of immune checkpoint inhibitors (anti–PD-1 or anti–CTLA-4) led to long-lasting immunologic memory in some of the irradiated mice receiving the dual blockade of activin A and TGFβ. Analysis of a public RNA sequencing (RNA-seq) dataset of patients with breast cancer from The Cancer Genome Atlas (TCGA) revealed that *INHBA* expression (gene encoding for activin A) was correlated with a tumor-infiltrating Treg signature (TITR) among 1,079 breast cancer cases analyzed, supporting the clinical relevance of this regulatory mechanism in patients with breast cancer. Consequently, these observations support a cross-talk between TGFβ and activin A that promotes Treg-mediated immunosuppression in breast cancer and suggest that targeting these two cytokines may be required to achieve durable immune responses, especially in the context of therapeutic strategies that combine immune checkpoint blockade and RT.

Materials and Methods

Mice

Six-week-old Balb/C female mice from Taconic Animal Laboratory were maintained under pathogen-free conditions in the animal facility at Weill Cornell Medicine. All experiments were approved by the Institutional Animal Care and Use Committee.

Cells and reagents

Balb/C mouse–derived breast carcinoma 4T1, as well as 67NR cells, were obtained from F. Miller (21), and TSA was provided by P.L. Lollini in 2002 (22). 4T1 is poorly immunogenic and highly metastatic, spreading systemically by the hematogenous route from the primary subcutaneous site, causing death of mice within 30 to 40 days due to lung metastases (23). TSA is poorly immunogenic and slowly metastasizes to the lungs, leading to gross metastases 60 to 80 days after initial injection at the primary subcutaneous site (24). 67NR is unable to metastasize (21). 4T1, TSA, and 67NR cells were authenticated in 2019 by IDEEX Bioresearch. MDA-MB-231 and MCF-7 human breast cancer cells were purchased from the ATCC in 2012. 4175-TR human breast cancers were obtained from J. Massagué in 2012. MDA-MB-231, MCF-7, and 4175-TR were authenticated in 2016 by IDEXX Bioresearch. Packaging cell HEK 293-FT was obtained from R.J. Schneider in 2012. All cells were further authenticated by morphology, phenotype, growth, and pattern of metastasis *in vivo* and routinely screened for *Mycoplasma* (LookOut Mycoplasma PCR Detection kit, Sigma-Aldrich). None of the cells used are listed in the International Cell Line Authentication Committee database of commonly misidentified cell lines. 4T1, TSA, 67NR, MDA-MB-231, MCF-7, 4175-TR, and HEK 293-FT were cultured in DMEM (GIBCO, Life Technologies) supplemented with L-glutamine (2 mmol/L, Life technology), penicillin (100 U/mL, Life Technology), streptomycin (100 μg/mL, Life Technologies), 2-mercapthoethanol (2.5×10^{-5} mol/L, Sigma-Aldrich), and 10% FBS (Life Technologies). For *in vitro* experiments, minimally passaged stock cells were freshly thawed and split maximum 3 times prior use. For *in vivo* experiments, minimally passaged stock cells were freshly thawed and split once prior to implantation. 1D11, a pan-isoform, TGFβ-neutralizing mouse mAb (200 μg/mouse; cat#BE0057), monoclonal anti-mouse CTLA-4 clone 9H10 (200 μg/mouse; cat#BE0131), and monoclonal anti-mouse PD-1 clone RMP1–14 (200 μg/mouse; cat#BE0146) were purchased from BioXCell. For experiments with doxycycline (Sigma-Aldrich), 0.5×10^6 cells were grown in media containing 10% of tetracycline-free FBS (Life Technologies) and induced with doxycycline (4 μg/mL) 5 days prior to treatment. Recombinant human interleukin-2 (rIL2) was obtained from the Biological Resources Branch, Developmental Therapeutics Program, Division of Cancer Treatment and Diagnosis, National Cancer Institute. Follistatin-288 (cat# 5836-FS-025/CF) and recombinant activin A (cat# 338-AC-500/CF) were purchased from R&D systems.

Lentiviral infection, shRNA-mediated gene knockdown, gene knock-in, and transduction

HEK 293-FT cells were used to produce viruses upon transfection of the packaging pPAX2 and envelope pMD2 plasmids (kindly provided by Dr. R.J. Schneider) and a pTRIPZ vector containing a tetracycline-inducible promoter (GE Dharmacon technology, kindly provided by Dr. R.J. Schneider). ShRNAs directed against activin A mRNA (*Inhba*, mouse-shRNA: TCCTTCCACTCAACAGTCATTA) or a nonsilencing sequence (NS; mouse-human-shRNA: AATTCTCCGAACGTGTCACGT) were cloned into pTRIPZ using EcoRI and XhoI restriction sites. Note that 4×10^6 HEK 293-FT plated in a 10 cm dish were transfected with 1 mL of opti-MEM (Life Technologies) solution containing 58 μL of Lipofectamine 2000 (Life Technology), 8 μg of pPAX2, 4 μg of pMD2, and 25 μg of pTRIPZ and incubated for 1 minute at 37°C; after which, 5 mL of opti-MEM was gently added onto the plate for 6 hours at 37°C. After the incubation, the transfecting solution was carefully removed and replaced by 6 mL of complete medium (described in Cells and Reagents section). Supernatants containing the lentiviruses were collected at 24 and 48 hours of incubation. PEG-*it* virus precipitation solution (5X, System Biosciences) was used to precipitate the lentivirus in 1 mL. Next, 0.5×10^6 4T1 cells were transduced with 1 mL of lentivirus diluted with 9 mL of complete medium (as described in Cells and Reagents section) for 48 hours. After the incubation time, cells were selected with fresh complete medium containing puromycin (4 μg/mL, Life Technologies) for an additional 48 hours. In some settings, the pTRIPZ plasmid was modified to insert the mouse *Inhba* cDNA under the tetracycline-inducible promoter using AgeI and MluI restriction sites and used to enforce the expression of activin A in TSA-transduced cells ($TSA^{KI\ Inhba}$). Methods of transfection, transduction, and selection to insert the knock-in construct in TSA cells were similar to the protocol described above.

Tumor challenge and treatment

For the 4T1 model, mice were injected s.c. in the right flank with 5×10^4 4T1 cells or its derivatives ($4T1^{shNS}$; $4T1^{shInhba}$) on day 0. For the TSA model, mice were injected s.c. with 1×10^5 TSA cells or its derivatives ($TSA^{KI\ Inhba}$) in the right flank (primary tumor) on day 0. On day 2, 1×10^5 parental TSA cells were injected s.c. in the left flank (secondary tumor). Perpendicular tumor diameters were measured with a Vernier caliper twice a week, and tumor volumes calculated as length × width^2 × 0.52. When applicable, gene knockdown or knock-in expression was induced by adding doxycycline at 100 μg/mL (20 mg/kg/day) into the mouse drinking water at day 8 after tumor establishment. Doxycycline was replenished every 4 days until day 26. On day 12, when tumors reached 60 to 80 mm^3, mice were randomly assigned to treatment groups. Local RT was given as previously described with some modifications (23). Briefly, all mice (including mice receiving sham RT) were with isoflurane (VWR). 4T1 or TSA primary tumors were irradiated with a 6 Gy dose given on days 13, 14, 15, 16, and 17 at a dose rate of 2.77 Gy/min using the Small Animal Radiation Research Platform (SARRP Xstrahl Ltd.). 1D11 mAb was administered i.p. (200 μg/mouse) every other day from day 12 to day 28. Anti–CTLA-4 was given i.p. (200 μg/mouse) on days 17, 20, and 23.

Anti–PD-1 was injected i.p. (200 μg/mouse) on days 18, 22, 26, and 30. On day 22, tumors and tumor-draining lymph nodes (TDLN) from 4T1 and TSA tumor-bearing mice were collected for flow cytometry analysis (see below) or *ex-vivo* restimulation with the tumor-specific MHC class I–restricted peptide AH1 (see below). In some experiments, mice that rejected the tumor completely and remained tumor-free for 100 days were rechallenged in the contralateral flank with 5×10^4 viable 4T1 cells and growth monitored. A group of naïve mice was challenged the same day as controls.

Measurement of activin A secretion

Note that 0.5×10^6 4T1, TSA, 67NR, 4175TR, MDA-MB-231, and MCF-7 were plated in a 10 cm dish containing 10 mL of complete medium. In some dish, TGFβ was blocked by adding 300 ng/mL of 1D11. After 24 hours, cells received a single dose of 6, 8, or 20 Gy at a dose rate of 2.85 Gy/min using the Small Animal Radiation Research Platform (SARRP Xstrahl Ltd.). Immediately after irradiation, medium was carefully removed and replaced by 6 mL of fresh complete medium containing 300 ng/mL of 1D11 when applicable. Supernatants and cells were collected after 24 hours to quantify activin A and count live cells by trypan blue (Life Technology), respectively. Activin A was measured in cell-free supernatants collected 24 hours after completion of tumor cell irradiation or 5 days after doxycycline induction using the human/mouse/rat Activin A Quantikine ELISA kit from R&D system (Cat# DAC00B). As per the manufacturer's instruction, 100 μL of undiluted supernatant (except for 4T1-derived supernatants, which were 2-fold diluted) and standards were assayed in triplicate wells. Optical densities were determined using a FlexStation 3 plate reader (Molecular Devices) set at 450 nm with 570 nm subtraction and standard curve generated using a log/log curve-fit. Measured concentrations were normalized by the number of live cells counted on an automated bright-field Cellometer AutoT4 (Nexcelom) to account for the proliferation arrest subsequent to RT.

Quantitative PCR with reverse transcription

Total RNA from 4T1 and their derivatives was extracted from lysates using TRIzol (ThermoFisher Scientific). Real-time PCR was performed using the Applied Biosystems 7500 real-time PCR cycler (ThermoFisher). One microgram of RNA was used for cDNA synthesis performed with the SuperScript VILO cDNA Synthesis Kit (ThermoFisher Scientific) followed by real-time RT-PCR with iTaq Universal SYBR Green Supermix (BioRad) according to manufacturer's protocol. Samples were normalized to the housekeeping gene *Rpl19*, and expression by untreated cells was assigned a relative value of 1.0. The PrimePCR SYBR Green assay primers (BioRad) used in this study were UniqueAssay ID: qMmuCID0006230 for mouse *Inhba* and qMmuCED0061753 for mouse *Rpl19*. Data were analyzed with the 7500 Dx Instrument's Sequence Detection software (ThermoFisher). To calculate the relative gene expression, the $2(-\Delta\Delta Ct)$ method was used.

Naïve $CD4^+$ T-cell isolation and coculture experiments

Naïve $CD4^+$ T cells were purified from spleens of healthy Balb/C mice with the naïve $CD4^+$ T-cell isolation kit from Miltenyi Biotec (cat# 130–106–643). Cell populations were >98% pure as confirmed by FACS analysis. When indicated, 4T1 or TSA tumor cells (1×10^5/mL) were added in the upper chamber, and purified naïve $CD4^+$ T cells (2×10^6/mL) were added in the lower compartment of a transwell (Fisher Scientific, cat# 07–200165). Anti-CD3 (5 μg/mL, ThermoFisher Scientific, cat# 16–0031–86), anti-CD28 (5 μg/mL, ThermoFisher Scientific, cat# 16–0281–82), and rIL2 (10 U/mL) were added in the transwell. Follistatin-288, a natural inhibitor of activin A, was added to selected transwells (1 μg/mL). Additionally, 1D11 was added to selected transwell (300 ng/mL) to block TGFβ. As a positive control, recombinant activin A was added to the naïve $CD4^+$ T cells compartment (10 ng/mL). After 5 days of coculture, $CD4^+$ T cells were harvested and analyzed for expression of Foxp3 and CD25 in live $CD4^+$ T cells by flow cytometry analysis.

Flow cytometry analysis

4T1 and TSA tumors were harvested and digested using a mouse Tumor Dissociation Kit (cat# 130–096–730, Miltenyi Biotec) prepared as per the manufacturer's instructions and run on a Miltenyi gentleMACS Octo Dissociator with heaters using manufacturer's recommended preset program (37C_m_TDK1). The resulting cell suspensions were filtered using a 40-μm cell strainer, and red blood cells were lysed (RBC lysis buffer, Life technologies). Samples were counted and stained with eBioscience fixable viability dye eFluor 780 (cat# 65–0863–18, ThermoFisher Scientific) to exclude dead cells. All samples were incubated with purified anti-mouse CD16–32 (Fc Block, cat#14–0161–86, ThermoFisher Scientific) for 15 minutes at 4°C prior surface staining. Surface antibody staining was performed for 30 minutes at 4°C, followed by a fixation/permeabilization for 30 minutes at 4°C (Transcription Factor Staining buffer set, ThermoFisher Scientific, cat# 00–5523–00). Finally, cells were stained for the intracellular factor FoxP3 for 30 minutes at 4°C. The following antibodies, all purchased from ThermoFisher Scientific, were used in the indicated dilution: fixable viability dye eFluor 780 (1:1,000, cat# 65–0863–18), CD8α-APC (1:100; cat#17–0081–83), CD4-Alexa Fluor 700 (1:100; cat#56–0041–82), CD45-PE-fluor 610 (1:100, 61–0451–82), FoxP3-PE (1:100, cat#12–4771–82), and CD25-efluor 450 (cat# 48–0251). Counting beads (CountBright absolute counting beads for flow cytometry, ThermoFisher Scientific) were used to determine absolute number of live $CD45^+CD4^+CD25^+FoxP3^+$ cells. All samples were acquired with LSRII or MACSQuant Analyzer 10 flow cytometers, and analyzed with FlowJo software version 10.4.0 (Tree Star) and a multistep gating strategy to identify immune cells (Supplementary Fig. S1).

Analysis of IFNγ production by $CD8^+$ T cells

Note that 5×10^5 4T1 or TSA-draining lymph node (TDLN) cells were cultured in RPMI1640 medium supplemented with 10% FBS (Life Technologies), $_L$-glutamine (2 mmol/L, Life Technologies), penicillin (100 U/mL, Life Technologies), streptomycin (100 μg/mL, Life Technologies), 2-mercaptoethanol (2.5×10^{-5} mol/L, Sigma-Aldrich), and with rIL2 (10 U/mL) in a 48-well plate and restimulated *ex vivo* with 1 μmol/L of the following peptides (GenScript): AH1A5 (SPSYAYHQF; referred as AH1), pMCMV (YPHFMPTNL) for 72 hours at 37°C as previously described (23). After incubation, cell-free supernatants were assessed for IFNγ concentration using the mouse IFNγ Quantikine ELISA kit (R&D Systems, cat# MIF00). As per the manufacturer's instructions, 50 μL of undiluted supernatant, standards, and recombinant mouse IFNγ (positive control) were assayed in triplicate wells. Optical densities were determined on a FlexStation 3 plate reader (Molecular Devices) set at 450 nm with 570 nm subtraction and standard curve generated using a log/log curve fit.

Gene expression analysis in human breast tumors

Tumor expression profiles of TCGA breast cancer (BRCA) dataset were analyzed in this study. Patient clinical data and level 3-processed RNA-seq data were downloaded from the Broad Genome Data

Analysis Center's FireBrowse resource (http://firebrowse.org/; TCGA data version 2016_01_28; ref. 25). RNA-seq data ("rnaseqv2") were generated via MapSplice alignment and RSEM quantitation as described (26, 27). BRCA cases were filtered to exclude male and gender "unknown" samples ($n = 13$), metastatic tissue samples ($n = 7$), and one errant skin cancer sample, yielding 1,079 female primary breast tumor samples for expression analysis. Intratumoral Treg abundance was quantified as a continuous variable using the geometric mean of the 108-gene signature of tumor-infiltrating Tregs (TITR score) reported by ref. 28 (Supplementary Dataset S6 of that publication). TGFβ signaling was quantified as a continuous variable using the geometric mean of the 80-gene TGFβ Response signature reported by ref. 29 and computed for the TCGA BRCA RNA-seq dataset by ref. 30 (Supplementary Table S1 of that publication). The cytolytic score was computed as the geometric mean of granzyme A (*GZMA*) and perforin (*PRF1*) expression values as previously described (31). Spearman's rank-order correlation analyses were conducted using SigmaPlot 12.0 (Systat Software Inc.).

Statistical analysis

All statistical analyses were performed using GraphPad Prism 7.0e. The identity of the statistical test performed, *P* values, and *n* values are stated in the figure legends. One-way ANOVA followed by Tukey *post hoc* comparisons was applied for statistical analysis of activin A secretion, IFNγ concentrations, percentage of cells, and CD8:Treg ratios. Longitudinal tumor growth data were analyzed using two-way ANOVA to assess overall group differences followed by Tukey *post hoc* comparisons. Survival was evaluated using the Kaplan–Meier model, and the log-rank Mantel–Cox test was used to compare treatment groups.

Results

Breast cancer cells secrete activin A in response to RT and TGFβ blockade

High circulating activin A in serum from patients with breast cancer has been associated with breast cancer progression and incidence of bone metastasis (32, 33). Because activin A can be produced by many cells at different levels (34, 35), multiple mouse and human breast cancer cell lines were tested *in vitro* for their ability to secrete activin A. All mouse breast cancer cells secreted activin A but at different levels, with the highest baseline secretion by 4T1 cells, a model of triple-negative breast cancer, and the lowest baseline secretion by TSA (**Fig. 1A**). Among human breast cancer cells, MDA-MB-231 cells, which are derived from a triple-negative tumor, secreted the highest activin A. An additional triple-negative human breast cancer cell line, 4175-TR, and the hormone receptor–positive human breast cancer cell line, MCF-7, both secreted lower activin A (**Fig. 1B**). This variability across murine and human breast cancer subtypes suggests that activin A secretion is independent from the subtype of breast cancer. Treatment of the breast cancer cells with RT significantly increased activin A secretion in a dose-dependent fashion for most the breast cancer cells

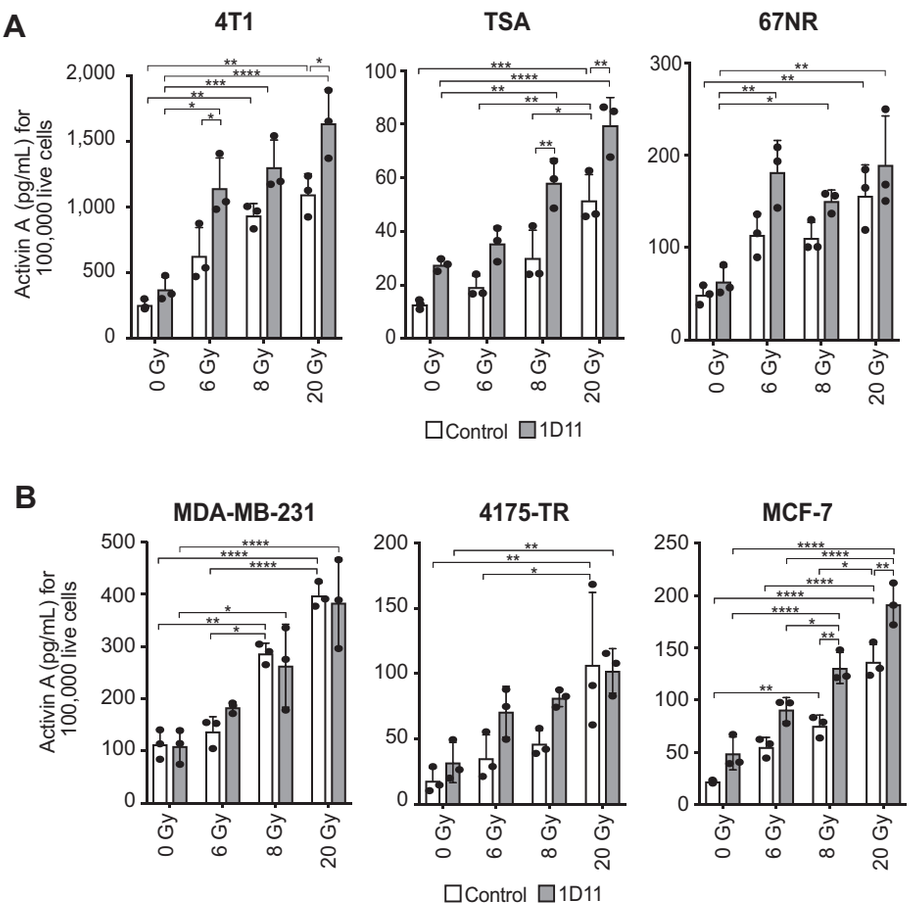

Figure 1.
Activin A is secreted by breast cancer cells and is increased in response to RT and TGFβ blockade. Murine breast cancer cells 4T1, TSA, and 67NR (**A**) and human breast cancer cells MDA-MB-231, 4175-TR, and MCF-7 (**B**) were treated with the pan–isoform-neutralizing TGFβ (1D11) antibody for 24 hours and irradiated with various doses, as indicated. Twenty-four hours following RT, secreted activin A was measured in supernatants by ELISA. Results are expressed in pg/mL ± SD for 100,000 live cells. One-way ANOVA followed by Tukey *post hoc* comparisons; *, $P < 0.05$; **, $P < 0.01$; ***, $P < 0.001$; and ****, $P < 0.0001$. Experiment was done in triplicate with $n = 3$/group.

lines tested (**Fig. 1**). The increase in activin A secretion was more pronounced when irradiated cells were incubated with the pan-isoform TGFβ-neutralizing mAb 1D11, an effect that was observed in the majority of the breast cancer investigated (**Fig. 1A** and **B**).

Tumor-derived activin A contributes to Treg increases in irradiated murine breast cancer

Activin A has been implicated in the induction of induced (i) Tregs in pathologic conditions including allergic diseases (13, 36). Thus, we hypothesized that the upregulation of activin A secretion by irradiated mammary carcinoma cells could contribute to the increase in Tregs associated with RT. To test this hypothesis, we first performed *in vitro* cocultures to determine if irradiated mammary carcinoma cells could induce the conversion of naïve $CD4^+$ T cells (defined as $CD62L^{hi}$) into iTregs (defined as $CD25^+FoxP3^+$) using the two mouse mammary carcinoma cells with the highest (4T1) and lowest (TSA) baseline secretion of activin A (**Fig. 1**). Recombinant activin A was used as a positive control. To separate the effects of TGFβ and activin A in iTreg induction, 1D11 and/or follistatin-288 (FS, a natural activin A inhibitor) were included in some cocultures. The number of $CD4^+$ T cells that acquired markers of iTregs was significantly increased by recombinant activin A (**Fig. 2**). Coculture with untreated or irradiated TSA or 4T1 breast cancer cells resulted in an increase of $CD4^+$ T cells acquiring markers of iTreg differentiation compared with naïve T cells alone. In cocultures with TSA cells, this increase in Tregs was abrogated by TGFβ blockade, whereas FS had no detectable effect, indicating that TGFβ played a dominant role in iTreg induction by cancer cells with low activin A expression (**Fig. 2B**). In contrast, TGFβ blockade enhanced, rather than reduced, iTregs when naïve $CD4^+$ T cells were cocultured with either untreated or previously irradiated high activin A–expressing 4T1 cells (**Fig. 2C**). Activin A blockade with FS did not have any effect on either untreated or previously irradiated 4T1 cells (**Fig. 2C**). We then reasoned that activin A and TGFβ could compensate each other to induce the conversion of Tregs *in vitro*. Supporting this hypothesis, a concomitant blockade of TGFβ and activin A effectively prevented iTreg generation induced by $CD4^+$ T cells in the presence of both untreated and irradiated 4T1 cells (**Fig. 2C**). Consequently, we concluded that TGFβ and activin A were both responsible for Treg conversion in high activin A–expressing breast cancer cells.

Next, to determine whether secretion of activin A at baseline in breast cancer similarly affected the tumor infiltration of Tregs *in vivo*, BALB/c mice bearing syngeneic low activin A–secreting TSA or high activin A–secreting 4T1 flank tumors were treated with i.p. injections of 1D11 or its isotype control every other day, starting at day 12 after tumor cell injection. Tumor-targeted RT was given in five daily fractions of 6 Gy (total dose 30 Gy), starting on day 13 (**Fig. 3A**). The choice of this RT dose and fractionation regimen was based on our prior experience with TGFβ blockade in these tumor models (23). Tumors were harvested at day 22 for analysis of tumor-infiltrating Tregs (**Fig. 3B**). In line with previous reports, RT increased Treg infiltration in both TSA and 4T1 tumors (**Fig. 3C** and **D**; refs. 4, 10). Consistent with *in vitro* results, TGFβ blockade reduced Tregs in untreated and irradiated TSA tumors (**Fig. 3C**), whereas it resulted in a significant increase in Tregs in untreated and irradiated 4T1 tumors (**Fig. 3D**).

To investigate if activin A secreted by 4T1 cells was responsible for the increase in Tregs observed upon TGFβ blockade *in vivo*, we used a genetic approach because pharmacologic inhibitors of activin A are not commercially available in sufficient quantity for *in vivo* use. To this end, 4T1 cells were transduced with a tetracycline-inducible shRNA targeting activin A mRNA (Supplementary Fig. S2A). Reduced secretion of activin A by $4T1^{sh\mathit{Inhba}}$ cells upon doxycycline induction was confirmed both at the gene and protein levels (Supplementary Fig. S2B and S2C). Next, mice were injected with control cells transduced with a nonsilencing construct, $4T1^{shNS}$ or $4T1^{sh\mathit{Inhba}}$ cells. Expression of shRNAs was induced once the tumors were established by administration of doxycycline. Mice were then treated with tumor-targeted RT and/or TGFβ blockade, and tumors were harvested for analysis at day 22 (**Fig. 4A**). Treg accumulation in mice bearing $4T1^{shNS}$ was significantly enhanced by TGFβ blockade (**Fig. 4B**). Conversely, in the 4T1 cells unable to secrete activin A, a decrease in intratumoral Tregs upon treatment with RT and TGFβ blockade was observed (**Fig. 4B**). Confirming our *in vitro* data, these results showed that dual blockade of activin A and TGFβ was required to prevent radiation-induced Treg accumulation in high activin A–expressing tumors.

Activin A limits priming of antitumor $CD8^+$ T cells after RT and TGFβ blockade

We have previously shown that TGFβ blockade during local RT induces $CD8^+$ T-cell responses to multiple endogenous tumor antigens in the 4T1 model of metastatic breast cancer (23). In light of the findings that this combination promoted an increase in intratumoral Tregs (**Figs. 3D** and **4B**), we hypothesized that inhibition of the activin A–induced Treg increase would further improve $CD8^+$ T-cell priming. To this end, TDLNs from mice implanted with $4T1^{shNS}$ and $4T1^{sh\mathit{Inhba}}$ cells treated with RT and TGFβ blockade were analyzed for IFNγ production in response to the tumor-specific MHC class I–restricted peptide AH1 (22). In line with our previous data, the $CD8^+$ T-cell response to AH1 was detected only in $4T1^{shNS}$-tumor bearing mice treated with the combination of RT and 1D11 (**Fig. 4C**). Activin A knockdown modestly induced $CD8^+$ T-cell reactive to AH1 in the presence of RT, but this effect was significantly enhanced by blockade of TGFβ (**Fig. 4C**). Dual targeting of TGFβ and activin A also enhanced the CD8:Treg ratio in irradiated 4T1 tumors (**Fig. 4D**).

Dual TGFβ and activin A blockade with RT induces durable tumor control

A high intratumoral ratio of effector $CD8^+$ T cells to Tregs has been previously shown to reflect successful antitumor immunity (37). To test the therapeutic antitumor activity of dual blockade of activin A and TGFβ with RT, mice were injected with $4T1^{shNS}$ and $4T1^{sh\mathit{Inhba}}$ cells. Activin A knockdown was induced once the tumors were established with doxycycline. Mice were then treated with local RT and/or TGFβ blockade and followed for tumor growth and survival. In the absence of RT, single or double blockade of TGFβ and activin A did not have any effect on 4T1 tumor growth or mouse survival (**Fig. 4E–G**). As we have previously shown (23), RT alone delayed tumor progression but was unable to completely eliminate tumors. Radiation-induced tumor control and survival of animals bearing $4T1^{sh\mathit{Inhba}}$ was modestly, but significantly, improved compared with animals bearing $4T1^{shNS}$ tumors (**Fig. 4F** and **G**). TGFβ blockade combined with local RT was able to induce initial complete tumor regression, but all tumors regrew after day 36. In contrast, the dual blockade of TGFβ and activin A completely eliminated the irradiated tumor in 57% of the mice, resulting in a significant increase in survival compared with all other groups (**Fig. 4E–G**). However, because most mice did not survive past day 75, immune memory was not established. Altogether, these results show that tumor-derived

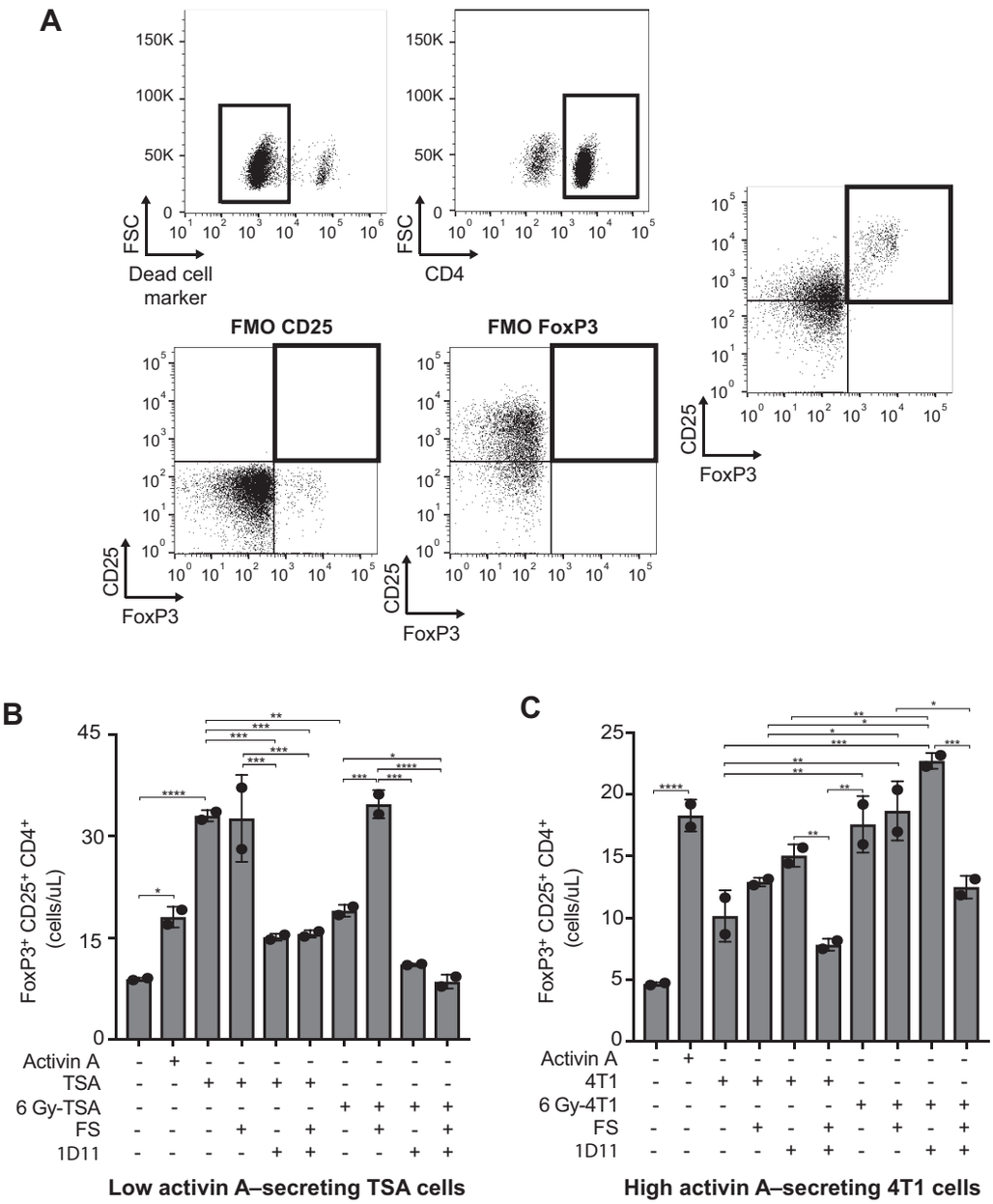

Figure 2.

Tumor-derived activin A promotes CD4$^+$ T-cell differentiation into iTregs *in vitro*. **A,** Gating strategy. FSC, forward scatter; FMO, fluorescence minus one. Naïve CD4$^+$ T cells isolated from spleens of Balb/c mice were cocultured with either untreated or 6 Gy–irradiated TSA (**B**) or 4T1 (**C**) breast cancer cells for 5 days. When applicable, blockade of activin A using follistatin-288 (FS) and/or TGFβ using 1D11 was performed. Percentages of naïve CD4$^+$ T cells converted into Tregs are expressed as FoxP3$^+$CD25$^+$ of CD4$^+$ live T cells (cell/μL) ± SD. One-way ANOVA followed by Tukey *post hoc* comparisons; *, $P < 0.05$; **, $P < 0.01$; ***, $P < 0.001$; and ****, $P < 0.0001$. Experiment was done in duplicate.

activin A limits the response of 4T1 tumors to focal RT and TGFβ blockade.

Immune checkpoint blockers improve RT and blockade of TGFβ and activin A

Despite the improved survival, only a small percentage of mice treated with RT and dual blockade of TGFβ and activin A were long-term survivors (**Fig. 4G**), an indication that additional interventions are needed to sustain antitumor responses. We have previously reported that the combination of TGFβ blockade with focal RT leads to adaptive immune resistance mediated by upregulation of PD-L1 in the tumor microenvironment and that administration of PD-1–blocking antibody extended mouse survival in this context (23). Blockade of CTLA-4 is also synergistic with focal RT in the 4T1 model (38). Thus,

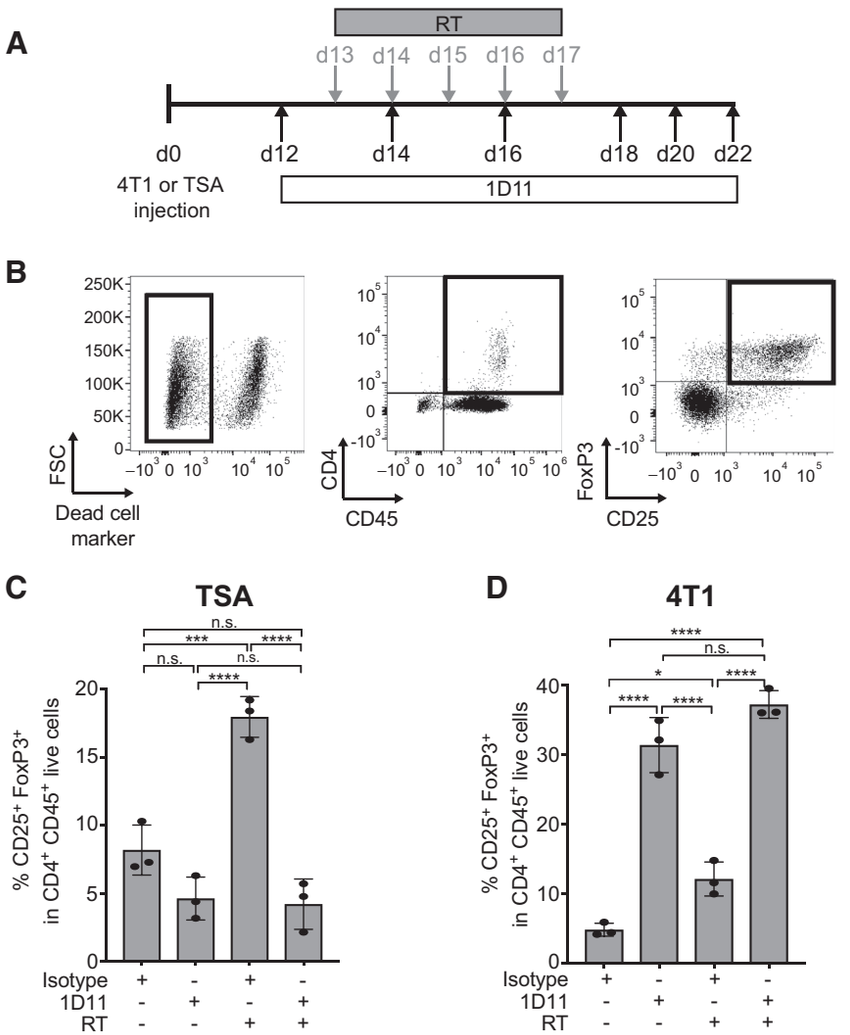

Figure 3.

TGFβ blockade promotes intratumoral Tregs in 4T1 but not in TSA tumors *in vivo*. **A,** *In vivo* experiment scheme. Syngeneic Balb/C mice received s.c. injection of 4T1 or TSA cells. The pan–TGFβ-neutralizing antibody 1D11 was given every other day starting day 12. RT was selectively given to s.c. tumors in five daily fractions of 6 Gy (5 × 6 Gy) on days (d)13, 14, 15, 16, and 17. On day 22, tumors were collected to analyze tumor-infiltrating Tregs, defined as $CD25^+FoxP3^+$ in $CD45^+CD4^+$ live cells. **B,** Flow cytometry gating strategy. FSC, forward scatter. Percentages of $FoxP3^+CD25^+$ in $CD4^+$ live T cells ± SD in TSA (**C**) and 4T1 (**D**) tumors. Each dot represents 1 animal. One-way ANOVA followed by Tukey *post hoc* comparisons; n.s., nonsignificant; *, $P < 0.05$; **, $P < 0.01$; ***, $P < 0.001$; and ****, $P < 0.0001$. Experiment was done in duplicate with $n = 3$ per group.

we asked whether the addition of immune checkpoint inhibitors would improve survival of mice treated with RT and the dual targeting of TGFβ and activin A. Mice bearing $4T1^{shNS}$ or $4T1^{sh\mathit{Inhba}}$ tumors were given doxycycline to knockdown activin A expression, then treated with focal RT, anti-TGFβ, anti–PD-1, and/or anti–CTLA-4 as indicated in **Fig. 5A**. In mice bearing $4T1^{sh\mathit{Inhba}}$ tumors, RT and TGFβ blockade induced complete tumor regression that was durable in 50% of the animals (**Fig. 5B** and **C**). The addition of anti–CTLA-4 or anti–PD-1 prevented tumor recurrence in 100% and 80% of the mice, respectively (**Fig. 5C**). Mice from all groups that remained tumor-free until day 100 were rechallenged with a tumorigenic inoculum of 4T1 cells together with a control group of 5 naïve mice. All 5 naïve mice developed tumors and succumbed to the disease by day 31. Two of 5 surviving mice from the $4T1^{sh\mathit{Inhba}}$+RT+1D11 group and 5 of 10 surviving mice from the $4T1^{sh\mathit{Inhba}}$+RT+anti–CTLA-4 group were protected. Only 1 of 8 survivors from $4T1^{sh\mathit{Inhba}}$+RT+anti–PD-1 was protected (**Fig. 5D**). Overall, these results showed that a multiprolonged approach that includes RT, immune checkpoint blockade, and inhibition of immune suppressive cytokines TGFβ and activin A is effective against very aggressive 4T1 tumors. However, they also suggest that long-term memory responses are induced by anti–CTLA-4 but not anti–PD-1 therapy.

Activin A knock-in increases Tregs and hinders abscopal responses in TSA-bearing mice

To further confirm the role of activin A in Treg induction, we tested if enforced increase in activin A secretion by TSA cells would result in reduced antitumor immune responses in mice treated with RT and TGFβ blockade. To this end, TSA cells were transduced with a plasmid expressing activin A cDNA under the control of a doxycycline-inducible promoter ($TSA^{KI\ \mathit{Inhba}}$; Supplementary Fig. S3A). Activin A quantification by ELISA confirmed an increased secretion of activin A by $TSA^{KI\ \mathit{Inhba}}$ upon doxycycline treatment (Supplementary Fig. S3B).

Next, mice were injected with $TSA^{KI\ \mathit{Inhba}}$ on day 0 in the right flank (primary site) and with parental TSA cells on day 2 in the contralateral flank (secondary site) to evaluate responses outside the RT field (i.e., abscopal effects). Half of the mice were fed doxycycline 4 days before treatment, with focal tumor RT delivered to the primary site and/or TGFβ blockade. Three mice per group were euthanized at day 22 to analyze primary tumors and TDLNs (**Fig. 6A**). In the absence of doxycycline treatment, TGFβ blockade was able to completely abrogate the radiation-induced Treg increase (**Fig. 6B**). Upregulation of activin A by doxycycline led to a mild but significant increase in intratumoral Tregs, which was

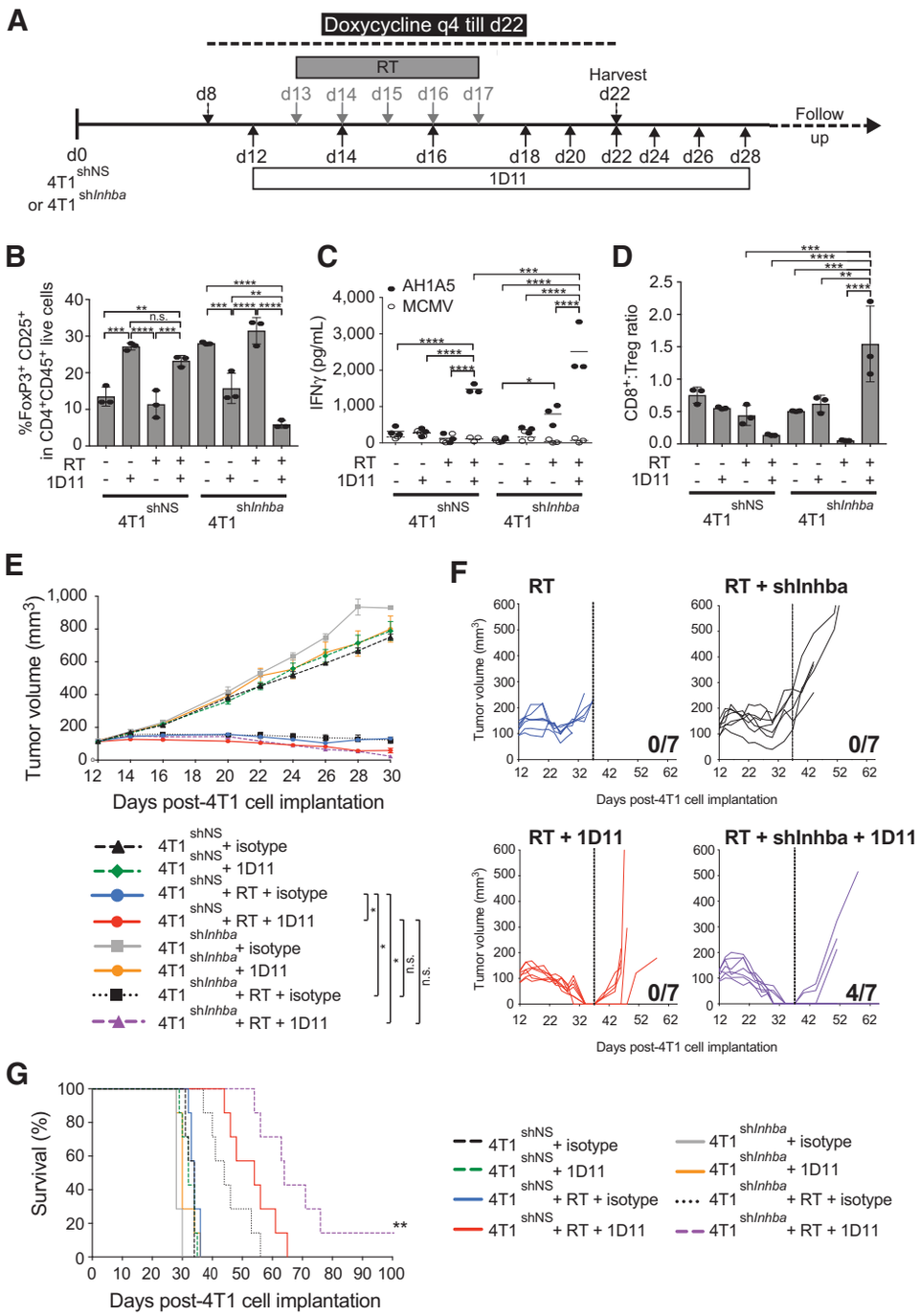

Figure 4.

Silencing tumor-derived activin A improves 4T1 tumor rejection and survival in mice treated with local RT and TGFβ blockade. **A,** Experiment scheme. 4T1$^{sh\mathit{Inhba}}$ or 4T1^{shNS} were injected s.c. into Balb/C mice on day 0. On day 8, mice were fed with doxycycline to silence the expression of the *Inhba* gene in 4T1 cells. Starting on day 12, 1D11 was given every other day. RT was selectively given to s.c. tumors in five daily fractions of 6 Gy (5 × 6 Gy) on days (d)13, 14, 15, 16, and 17. **B–D,** On day 22, tumors and TDLNs were collected for immune analysis in 4T1 tumor–bearing animals. Frequency of Tregs [FoxP3$^+$CD25$^+$ in live CD45$^+$ CD4$^+$ T cells (cell/μL ± SD)] in 4T1 tumors (**B**; $n = 3$/group), and IFNγ production by TDLN cells in response to the CD8$^+$ T-cell epitope AH1 (full circles) or control peptide MCMV (**C**; open circles). Horizontal lines indicate the mean of antigen-specific (solid lines) or control (dashed lines) IFNγ concentration and 4T1 tumor–infiltrating CD8:Treg ratios (**D**). **B–D,** Each symbol represents 1 animal. One-way ANOVA followed by Tukey *post hoc* comparisons; n.s., nonsignificant; *, $P < 0.05$; **, $P < 0.01$; ***, $P < 0.001$; and ****, $P < 0.0001$. Experiment was done in duplicate with $n = 3$ per group. Mean tumor growth (**E**), individual tumor growth (**F**), and survival (**G**) of mice bearing 4T1^{shNS} or 4T1$^{sh\mathit{Inhba}}$ tumors treated with RT and/or the TGFβ blockading antibody 1D11. **E** and **F,** Two-way ANOVA followed by Tukey *post hoc* comparisons; n.s., nonsignificant and *, $P < 0.05$. Experiment was done in duplicate with $n = 7$/group. **G,** Survival by log-rank (Mantel–Cox) test; **, $P < 0.01$. Experiment was done in duplicate with $n = 7$/group.

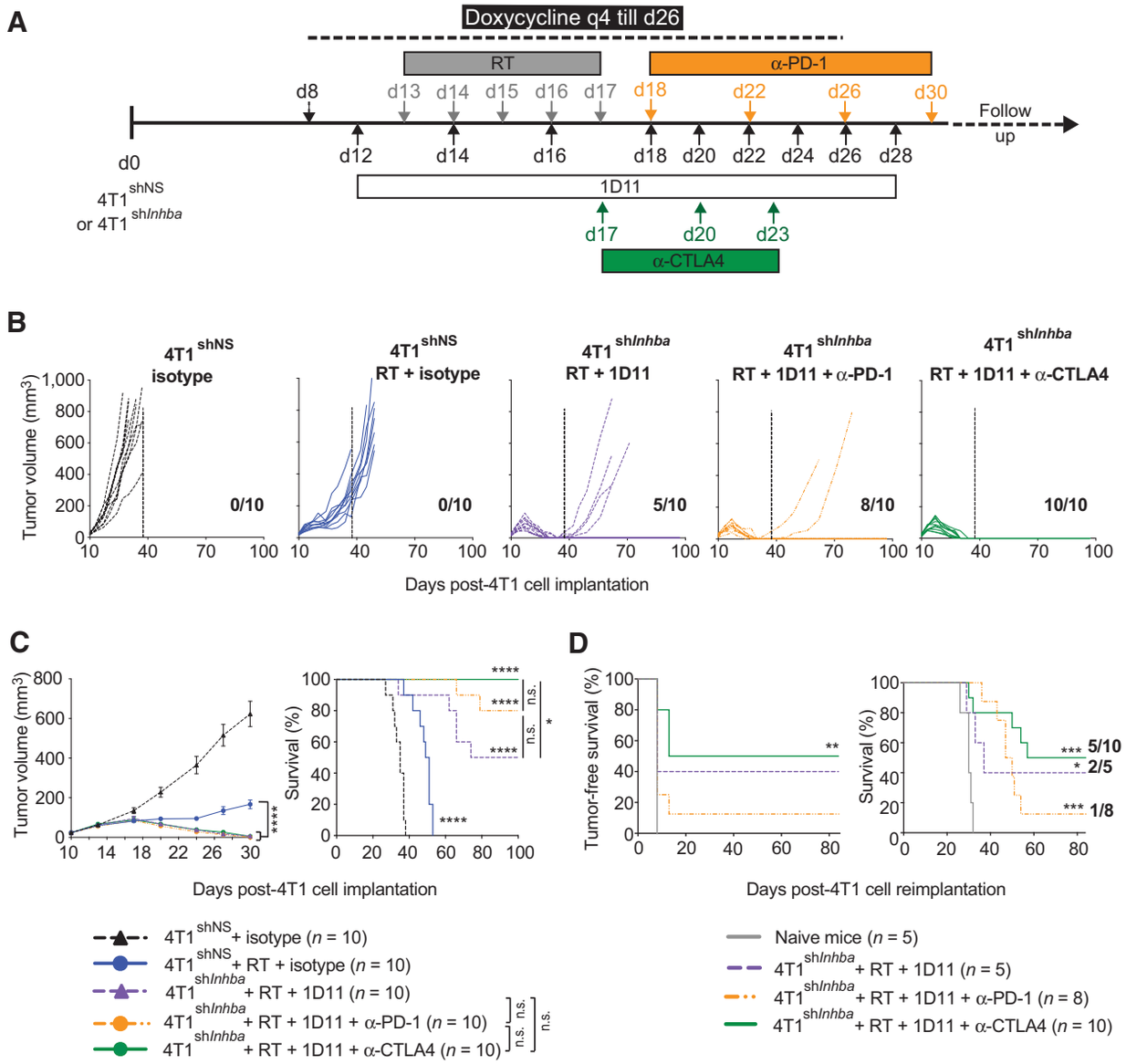

Figure 5.

Dual blockade of TGFβ and activin A is required to generate long-lasting immune memory in irradiated mice treated with immune checkpoint blockade. **A,** Experiment scheme. $4T1^{shInhba}$ or $4T1^{shNS}$ were injected s.c. into Balb/C mice on day 0. On day 8, mice were fed with doxycycline to silence the expression of the *Inhba* gene in 4T1 cells. Starting on day 12, 1D11 was given every other day. RT was selectively given to s.c. tumors in five daily fractions of 6 Gy (5 × 6 Gy) on days (d)13, 14, 15, 16, and 17. When applicable, anti–CTLA-4 was administered on days 17, 20, and 23, and anti–PD-1 was given on days 18, 22, 26, and 30. Individual (**B**) and mean (**C**) tumor growth and survival of mice bearing $4T1^{shNS}$ or $4T1^{shInhba}$ tumors. **B** and **C,** Tumor growth: $n = 10$/group; ****, $P < 0.0001$; two-way ANOVA followed by Tukey *post hoc* comparisons. Survival: $n = 10$/group; n.s., nonsignificant; *, $P < 0.05$; and ****, $P < 0.0001$; log-rank (Mantel–Cox) test. **D,** Tumor-free survival and survival of mice from $4T1^{shInhba}$ + RT + 1D11 ($n = 5$; dashed purple), $4T1^{shInhba}$ + RT + 1D11 + anti–PD-1 ($n = 8$; dashed orange), and $4T1^{shInhba}$ + RT + 1D11 + anti–CTLA-4 ($n = 10$; green) that cleared tumors and were rechallenged at day 100 with a tumorigenic inoculum of 4T1 cells, together with a group of naïve mice ($n = 5$; gray). *, $P < 0.05$; **, $P < 0.01$; and ***, $P < 0.001$; log-rank (Mantel–Cox) test.

enhanced by RT and was not affected by TGFβ blockade (**Fig. 6B**). Upregulation of activin A by doxycycline abrogated $CD8^+$ T-cell responses to the tumor-specific epitope AH1 in the TDLNs of mice treated with RT and TGFβ blockade (**Fig. 6C**). Consistent with reduced activation of antitumor $CD8^+$ T cells in doxycycline-fed mice, the contralateral nonirradiated tumor continued to grow during RT and TGFβ blockade, whereas in the absence of enforced activin A upregulation, significant inhibition of the secondary tumor was induced by treatment with RT and TGFβ blockade (**Fig. 6D** and **E**), as we previously reported (23). Overall, these results confirm a critical role for activin A as a regulator of antitumor immune responses induced by RT.

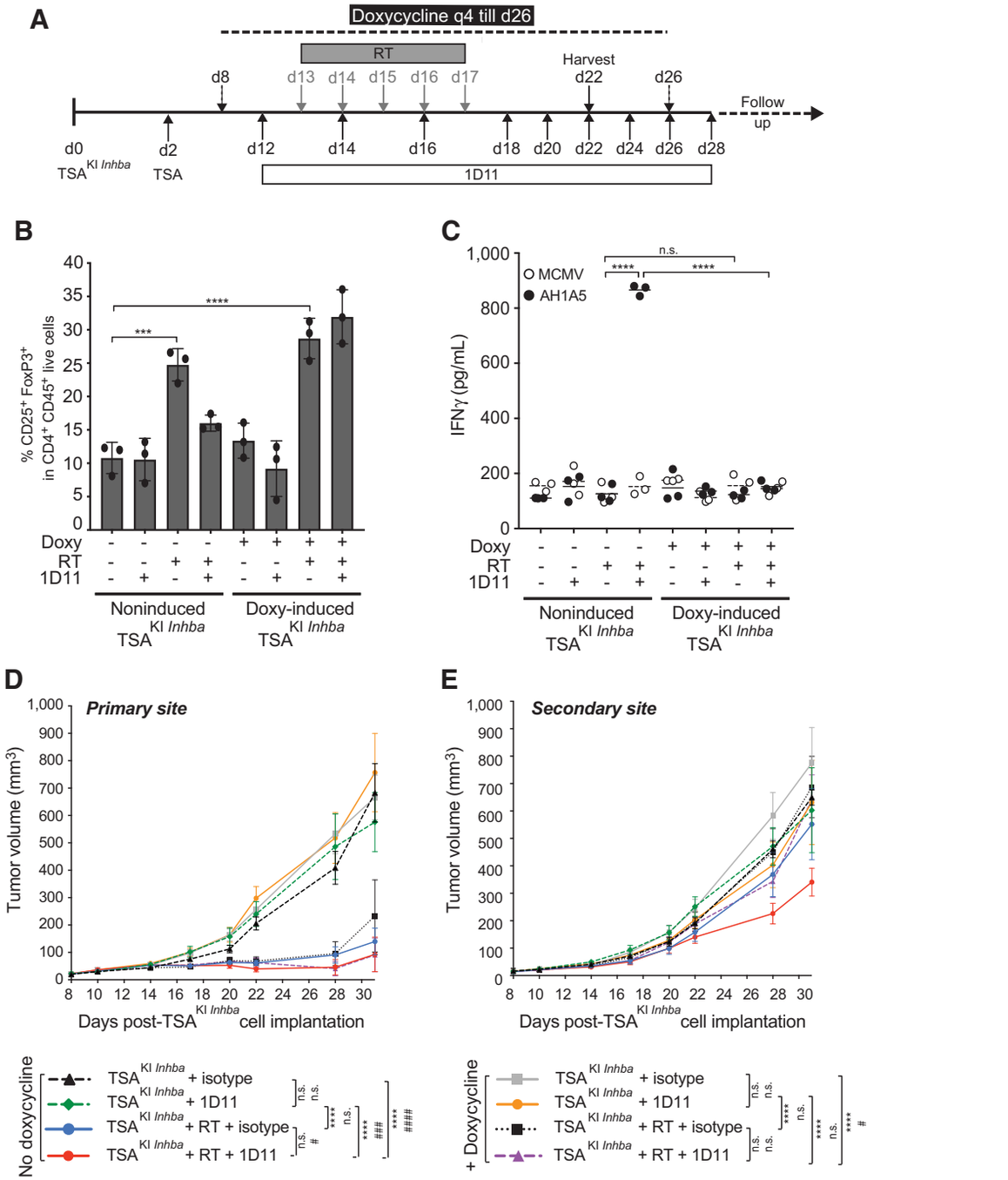

Figure 6.

Enforced secretion of activin A abrogates abscopal responses in TSA tumor–bearing animals treated with local RT and TGFβ blockade. **A,** Experiment scheme. Half of the mice with tetracycline-inducible *Inhba* in TSA ($TSA^{KI\ Inhba}$) in the primary tumor and parental TSA in the secondary tumor were given doxycycline. In some mice, five daily fractions of 6 Gy were selectively administered to the primary tumor combined with TGFβ blockade. On day (d)22, 3 mice per group were euthanized to harvest tumors and TDLNs for immune analysis. **B,** Percentages of $FoxP3^+CD25^+$ in live $CD45^+CD4^+$ T cells (% ± SD) in TSA tumors ($n = 3$/group). **C,** IFNγ secretion by TDLN cells in response to the $CD8^+$ T-cell epitope AH1 (full circles) or control peptide MCMV (open circles; $n = 3$/group). **B** and **C,** Each symbol represents 1 animal. One-way ANOVA followed by Tukey *post hoc* comparisons; n.s., nonsignificant; *, $P < 0.05$; **, $P < 0.01$; ***, $P < 0.001$; and ****, $P < 0.0001$. Mean tumor growth of the irradiated (**D**) and abscopal (**E**) tumors in mice treated with isotype (dashed back line), isotype + doxycycline (gray line), 1D11 (dashed green line), 1D11 + doxycycline (orange line), RT + isotype (blue line), RT + isotype + doxycycline (dotted back line), RT + 1D11 (red line), or RT + 1D11 + doxycycline (dashed purple line). **D** and **E,** Longitudinal primary tumor growth data were analyzed using two-way ANOVA to assess overall group differences, followed by Tukey *post hoc* comparisons; n.s., nonsignificant and ****, $P < 0.0001$; comparison of abscopal tumor growth, two-way ANOVA followed by Tukey *post hoc* comparisons; n.s., nonsignificant; #, $P < 0.05$; ###, $P < 0.001$; and ####, $P < 0.0001$. Duplicate experiment with $n = 7$/group.

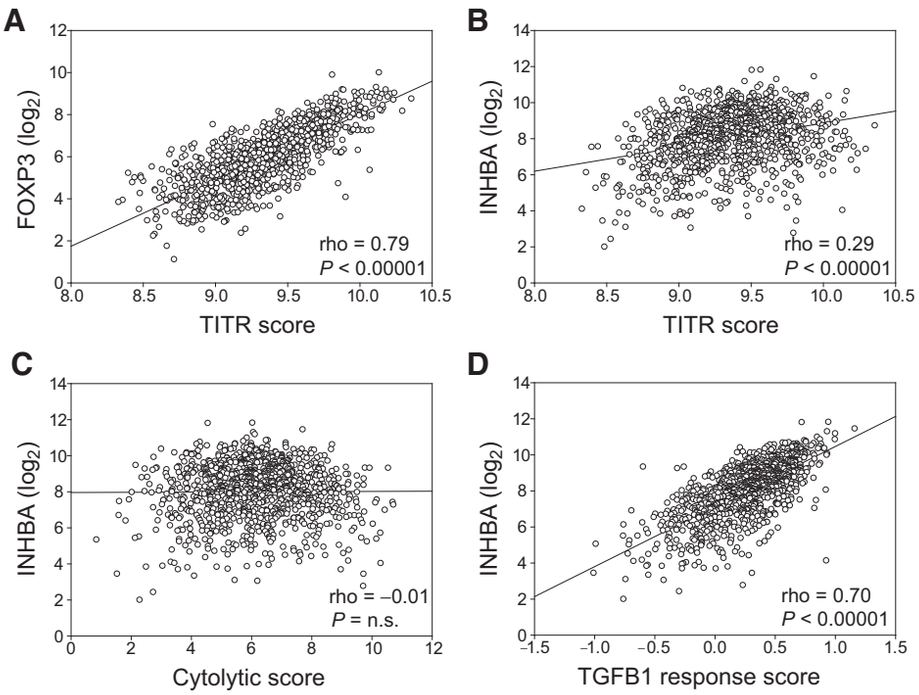

Figure 7.
INHBA expression correlates with the tumor-infiltrating Treg score in patients with breast cancer. Positive correlation between FOXP3 (**A**) and *INHBA* (**B**) with the TITR score. **C,** Correlation between *INHBA* and the cytolytic score. n.s., nonsignificant. **D,** Positive correlation between *INHBA* and the TGFβ response score. Results are illustrated in scatter plot from the RNA-seq TCGA dataset of breast cancer ($n = 1{,}079$). *P* values represent the statistical results of the Pearson correlation analysis.

INHBA expression correlates with the tumor-infiltrating Treg score in patients

To test whether activin A expression in human breast cancer may lead to enhanced Treg infiltration into tumors, we took advantage of TCGA RNA-seq BRCA public dataset to investigate the relationships between *INHBA* (gene encoding for the activin A protein; ref. 39), the abundance of Tregs, and TGFβ signaling. First, the abundance of Tregs was estimated using a robust tumor-agnostic gene signature of tumor-infiltrating Tregs (TITR signature; $n = 108$; defined by ref. 28) and considered the geometric mean of these genes as a continuous score for TITR. We then confirmed that this gene signature was reflecting intratumoral Tregs by investigating the correlation between the TITR score and *FOXP3* expression, a Treg-specific transcription factor (**Fig. 7A**; ref. 40; rho = 0.79; $P < 0.0001$). Having demonstrated that the TITR score was a reliable tool to estimate Treg infiltration in breast tumors, we then asked whether *INHBA* expression was associated with Treg abundance. Consistent with our preclinical observations, we found that *INHBA* was significantly associated with the TITR signature (**Fig. 7B**), but did not correlate with an effector cytolytic gene signature (**Fig. 7C**; ref. 31). A correlation between *INHBA* expression and *TGFB1* response signature (defined by ref. 29) was observed (**Fig. 7D**), thus supporting a cross-talk between activin A and TGFβ in human breast cancer. When the dataset was stratified for ER^+ and ER^- tumors, the positive correlation between *INHBA* and the Treg signature remained significant ($P < 0.0001$ in both ER^+ and ER^- tumors; Supplementary Fig. S4), therefore indicating that the correlation between *INHBA* and the TITR signature was independent of ER status and may reflect a mechanism of immune evasion that was independent from breast cancer tumor subtypes. Overall, these data were consistent with our preclinical findings and support the relevance of targeting activin A in human breast cancer to decrease Treg-mediated immunosuppression.

Discussion

Treg-mediated immunosuppression plays an important role in protecting tumors from immune rejection. Therefore, multiple therapeutic strategies are being tested to target Tregs, but effective ways to deplete Tregs in the TME of patients with cancer remain elusive. Several agents directed to TGFβ have been tested in preclinical and clinical studies for the ability to elicit immune-mediated tumor rejection (41), and in some studies, a reduction in Tregs is reported (42). Here, we showed that the ability of TGFβ blockade to reduce Treg numbers was dependent on baseline activin A secreted by the cancer cells. In the context of RT, TGFβ blockade was effective at abrogating the increased Treg infiltration in TSA tumors that secrete very low amounts of activin A. In the 4T1 tumor model, which has high baseline expression of activin A, TGFβ blockade had the paradoxical effect of further increasing Tregs *in vitro* and *in vivo* compared with untreated controls after RT. These results have important implications for the use of TGFβ inhibitors in the clinic and suggest that the ability of the treatment to reduce the immune suppressive TME may depend on the intrinsic ability of the cancer cells to secrete activin A at levels required to induce Tregs.

Our study was limited to mammary carcinomas, and we found that all of the human and mouse breast cancer cells tested secreted activin A, albeit at variable levels. Because activin A secretion was enhanced by RT, it will be important to measure this cytokine in patients with breast cancer undergoing RT. In a prior trial testing the combination of focal RT and TGFβ blockade by the antibody fresolimumab in patients with metastatic breast cancer, no objective abscopal responses were observed. However, overall survival was significantly longer in the arm receiving the higher dose of fresolimumab (43). It is intriguing to consider if an increased Treg representation in irradiated tumors contributes to impaired priming of antitumor T cells, thus explaining the lack of objective abscopal responses in this cohort. Although the

trial did not require on-treatment or posttreatment tumor tissue for analysis, sequential blood specimens were obtained, demonstrating that in some patients, Tregs are increased in the peripheral blood (43).

Activin A is a member of the TGFβ family with pleiotropic effects that was shown to promote a protumorigenic immune infiltrate. The induction of immune-suppressive Tregs by activin A has been previously described in asthma, where allergen-specific Tregs suppress Th2-mediated allergic reactions (13, 14). Here, we showed that activin A promotes Tregs in cancer and hampers antitumor immune responses induced by RT and TGFβ blockade. We also found that either activin A silencing or TGFβ blockade increased Tregs in 4T1 tumor, which secretes high baseline activin A. As a result, it is conceivable that activin A and TGFβ cooperate in maintaining a high number of Tregs in the breast cancer TME.

Activin A and TGFβ share structural similarities (44) and the SMAD2/3 signal transduction pathway (45). There is at least some evidence that activin A can increase TGFβ1-induced FoxP3 expression in T cells *in vitro* (46). We observed a "compensatory" increase in activin A when TGFβ was blocked, suggesting the existence of a cross-talk between these two TGFβ family members. Similar findings have been reported in vascular development where the knockdown of the TGFβ type-I receptor (aka ALK5, TGFBR1) in E9.5 embryos resulted in the upregulation of the activin A/ALK4 pathway to counterweigh the absence of SMAD2/3 phosphorylation (15).

In the 4T1 model, dual blockade of activin A and TGFβ improved the responses in irradiated tumors in some mice, but long-term (>100 days) survival was rare. TGFβ is a barrier to radiation-induced activation of antitumor immune responses, but blocking TGFβ is insufficient to generate robust and sustained antitumor immunity in both mice and in patients with breast cancer (23, 43). In mice, upregulation of PD-L1 and PD-L2 on 4T1 cancer cells and intratumoral myeloid cells after treatment with RT and TGFβ blockade is a mechanism limiting tumor rejection (23). Thus, it is likely that multiple barriers need to be targeted in the 4T1 mouse tumors, which behave like aggressive and poorly immunogenic human breast cancer, to improve responses to immunotherapy. This concept is consistent with the overall low response rate to treatment with PD-1/PD-L1–targeting antibodies observed in patients with breast cancer (47). Here, we demonstrated that the combination of RT, dual blockade of TGFβ and activin A, and CTLA-4 inhibition could lead to complete tumor regression and long-term survival in all mice bearing 4T1 tumors, and in 50%, there was a long-lived protective memory response. Similar improvement in long-term survival was observed when anti–PD-1 was used in place of anti–CTLA-4, but only 12.5% of the mice developed long-lived protective memory responses, an observation that will require further investigation.

The clinical relevance of our findings remains to be investigated. However, it is plausible that increased activin A could contribute to limiting the efficacy of TGFβ pathway inhibitors, at least in some patients (16, 41, 43). Supporting this notion, our retrospective analysis of the public TCGA BCRA dataset revealed a significant correlation between *INHBA* expression, TGFβ signaling, and Treg infiltration. With the limitations pertaining to retrospective *in silico* studies, our findings suggest that activin A may be an actionable target to reduce immunosuppression in patients with irradiated breast cancer, possibly independently from the breast cancer subtype, as demonstrated by the absence of differential expression of *INHBA* between ER^+ and ER^- cases. Thus, activin A inhibitors could enhance the response to RT in patients with high activin A–expressing breast cancer. Although no activin A inhibitor is currently available for clinical use, STM 434 (a soluble receptor ligand trap targeting activin A) is under clinical investigation for the treatment of ovarian cancer. Data from the first-in-human phase I trial show a lack of clinical response (48). It is possible that activin A blockade might be effective only as a component of a multi-prolonged therapy that includes TGFβ inhibitors and RT, and possibly CTLA-4 blockade.

High expression of activin A has been described in other solid malignancies such as esophageal and non–small cell lung cancers (39, 49). It is intriguing to consider if activin A baseline secretion could predict for limited clinical efficacy of ongoing clinical trials evaluating the dual blockade of TGFβ and PD-L1 in irradiated esophageal cancer and non–small cell lung cancer in ongoing clinical studies (NCT0481256, NCT03554473; source: www.clinicaltrials.gov) in the absence of activin A blockade. In conclusion, our results identified activin A as a player in the complex immune evasion of cancer and suggest that identifying and targeting multiple barriers may be necessary to enhance clinical responses to immunotherapy (50). Overall, these data highlight the role of cytokines belonging to the TGFβ family in shaping the TME and cancer progression, particularly in irradiated tumors. Although the role of activin A in increasing Tregs in patients with breast cancer remains to be confirmed, our data provide the rationale for testing this pathway in the clinic and provide a potential new actionable target to improve responses of patients with breast cancer to RT and immunotherapy combinations.

Authors' Disclosures

S.C. Formenti reports grants and personal fees from Merck, Bristol-Meyers Squibb, Varian, and Breast Cancer Research Foundation and personal fees from Bayer outside the submitted work. S. Demaria reports grants from NIH and Breast Cancer Research Foundation during the conduct of the study, as well as grants and personal fees from Lytix Biopharma, grants from Nanobiotix, and personal fees from EMD Serono and Mersana Therapeutics outside the submitted work. C. Vanpouille-Box reports grants from U.S. Department of Defense during the conduct of the study; other from EMD Serono outside the submitted work; and academic mentoring of a postdoctoral fellow with F. Hoffmann-La Roche Ltd (better known as Roche). No disclosures were reported by the other authors.

Authors' Contributions

M. De Martino: Data curation, formal analysis, investigation, methodology, writing–review and editing. **C. Daviaud:** Data curation, formal analysis, validation, methodology, writing–review and editing. **J.M. Diamond:** Data curation, formal analysis, writing–original draft, writing–review and editing. **J. Kraynak:** Data curation, investigation, writing–review and editing. **A. Alard:** Resources, data curation, writing–review and editing. **S.C. Formenti:** Conceptualization, funding acquisition, writing–review and editing. **L.D. Miller:** Formal analysis, validation, visualization, writing–review and editing. **S. Demaria:** Conceptualization, supervision, funding acquisition, visualization, writing–review and editing. **C. Vanpouille-Box:** Conceptualization, data curation, formal analysis, supervision, funding acquisition, validation, investigation, methodology, writing–original draft, project administration, writing–review and editing.

Acknowledgments

This work was supported by a postdoctoral fellowship from the U.S. Department of Defense (DOD) Breast Cancer Research Program (BCRP; W81XWH-13-1-0012) to C. Vanpouille-Box. Additional funding was provided by intramural start-up funds of C. Vanpouille-Box, the Breast Cancer Research Foundation BCRF-16-054 (to S.C. Formenti and S. Demaria), and by NIH R01 CA201246 to S. Demaria.

The costs of publication of this article were defrayed in part by the payment of page charges. This article must therefore be hereby marked *advertisement* in accordance with 18 U.S.C. Section 1734 solely to indicate this fact.

Received May 4, 2019; revised September 1, 2020; accepted October 14, 2020; published first October 22, 2020.

References

1. Ngwa W, Irabor OC, Schoenfeld JD, Hesser J, Demaria S, Formenti SC. Using immunotherapy to boost the abscopal effect. Nat Rev Cancer 2018;18:313–22.
2. Rodriguez-Ruiz ME, Vanpouille-Box C, Melero I, Formenti SC, Demaria S. Immunological mechanisms responsible for radiation-induced abscopal effect. Trends Immunol 2018;39:644–55.
3. Wennerberg E, Lhuillier C, Vanpouille-Box C, Pilones KA, Garcia-Martinez E, Rudqvist NP, et al. Barriers to radiation-induced in situ tumor vaccination. Front Immunol 2017;8:229.
4. Schaue D, Xie MW, Ratikan JA, McBride WH. Regulatory T cells in radiotherapeutic responses. Front Oncol 2012;2:90.
5. Kachikwu EL, Iwamoto KS, Liao YP, DeMarco JJ, Agazaryan N, Economou JS, et al. Radiation enhances regulatory T cell representation. Int J Radiat Oncol Biol Phys 2011;81:1128–35.
6. Horwitz DA, Zheng SG, Gray JD. Natural and TGF-beta-induced Foxp3(+)CD4(+) CD25(+) regulatory T cells are not mirror images of each other. Trends Immunol 2008;29:429–35.
7. Liu Y, Zhang P, Li J, Kulkarni AB, Perruche S, Chen W. A critical function for TGF-beta signaling in the development of natural CD4+CD25+Foxp3+ regulatory T cells. Nat Immunol 2008;9:632–40.
8. Barcellos-Hoff MH, Derynck R, Tsang ML, Weatherbee JA. Transforming growth factor-beta activation in irradiated murine mammary gland. J Clin Invest 1994;93:892–9.
9. Jobling MF, Mott JD, Finnegan MT, Jurukovski V, Erickson AC, Walian PJ, et al. Isoform-specific activation of latent transforming growth factor beta (LTGF-beta) by reactive oxygen species. Radiat Res 2006;166:839–48.
10. Muroyama Y, Nirschl TR, Kochel CM, Lopez-Bujanda Z, Theodros D, Mao W, et al. Stereotactic radiotherapy increases functionally suppressive regulatory T cells in the tumor microenvironment. Cancer Immunol Res 2017;5:992–1004.
11. Loomans HA, Andl CD. Activin receptor-like kinases: a diverse family playing an important role in cancer. Am J Cancer Res 2016;6:2431–47.
12. Antsiferova M, Werner S. The bright and the dark sides of activin in wound healing and cancer. J Cell Sci 2012;125:3929–37.
13. Semitekolou M, Morianos I, Banos A, Konstantopoulos D, Adamou-Tzani M, Sparwasser T, et al. Dendritic cells conditioned by activin A-induced regulatory T cells exhibit enhanced tolerogenic properties and protect against experimental asthma. J Allergy Clin Immunol 2018;141:671–84.
14. Tousa S, Semitekolou M, Morianos I, Banos A, Trochoutsou AI, Brodie TM, et al. Activin-A co-opts IRF4 and AhR signaling to induce human regulatory T cells that restrain asthmatic responses. Proc Natl Acad Sci U S A 2017;114:E2891–E900.
15. Carvalho RL, Itoh F, Goumans MJ, Lebrin F, Kato M, Takahashi S, et al. Compensatory signalling induced in the yolk sac vasculature by deletion of TGFbeta receptors in mice. J Cell Sci 2007;120:4269–77.
16. Staudacher JJ, Bauer J, Jana A, Tian J, Carroll T, Mancinelli G, et al. Activin signaling is an essential component of the TGF-beta induced pro-metastatic phenotype in colorectal cancer. Sci Rep 2017;7:5569.
17. Seder CW, Hartojo W, Lin L, Silvers AL, Wang Z, Thomas DG, et al. Upregulated INHBA expression may promote cell proliferation and is associated with poor survival in lung adenocarcinoma. Neoplasia 2009;11:388–96.
18. Bashir M, Damineni S, Mukherjee G, Kondaiah P. Activin-A signaling promotes epithelial-mesenchymal transition, invasion, and metastatic growth of breast cancer. NPJ Breast Cancer 2015;1:15007.
19. Carl C, Flindt A, Hartmann J, Dahlke M, Rades D, Dunst J, et al. Ionizing radiation induces a motile phenotype in human carcinoma cells in vitro through hyperactivation of the TGF-beta signaling pathway. Cell Mol Life Sci 2016;73:427–43.
20. Hardy CL, Rolland JM, O'Hehir RE. The immunoregulatory and fibrotic roles of activin A in allergic asthma. Clin Exp Allergy 2015;45:1510–22.
21. Aslakson CJ, Miller FR. Selective events in the metastatic process defined by analysis of the sequential dissemination of subpopulations of a mouse mammary tumor. Cancer Res 1992;52:1399–405.
22. Rosato A, Dalla Santa S, Zoso A, Giacomelli S, Milan G, Macino B, et al. The cytotoxic T-lymphocyte response against a poorly immunogenic mammary adenocarcinoma is focused on a single immunodominant class I epitope derived from the gp70 Env product of an endogenous retrovirus. Cancer Res 2003;63:2158–63.
23. Vanpouille-Box C, Diamond JM, Pilones KA, Zavadil J, Babb JS, Formenti SC, et al. TGFbeta is a master regulator of radiation therapy-induced antitumor immunity. Cancer Res 2015;75:2232–42.
24. Cavallo F, Di Carlo E, Butera M, Verrua R, Colombo MP, Musiani P, et al. Immune events associated with the cure of established tumors and spontaneous metastases by local and systemic interleukin 12. Cancer Res 1999;59:414–21.
25. Analysis-ready standardized TCGA data from broad GDAC Firehose 2016_01_28 run. Broad Institute of MIT and Harvard; 2016.
26. Li B, Dewey CN. RSEM: accurate transcript quantification from RNA-seq data with or without a reference genome. BMC Bioinformatics 2011;12:323.
27. Wang K, Singh D, Zeng Z, Coleman SJ, Huang Y, Savich GL, et al. MapSplice: accurate mapping of RNA-seq reads for splice junction discovery. Nucleic Acids Res 2010;38:e178.
28. Magnuson AM, Kiner E, Ergun A, Park JS, Asinovski N, Ortiz-Lopez A, et al. Identification and validation of a tumor-infiltrating Treg transcriptional signature conserved across species and tumor types. Proc Natl Acad Sci U S A 2018;115:E10672–E81.
29. Teschendorff AE, Gomez S, Arenas A, El-Ashry D, Schmidt M, Gehrmann M, et al. Improved prognostic classification of breast cancer defined by antagonistic activation patterns of immune response pathway modules. BMC Cancer 2010;10:604.
30. Thorsson V, Gibbs DL, Brown SD, Wolf D, Bortone DS, Ou Yang TH, et al. The immune landscape of cancer. Immunity 2018;48:812–30.
31. Rooney MS, Shukla SA, Wu CJ, Getz G, Hacohen N. Molecular and genetic properties of tumors associated with local immune cytolytic activity. Cell 2015;160:48–61.
32. Incorvaia L, Badalamenti G, Rini G, Arcara C, Fricano S, Sferrazza C, et al. MMP-2, MMP-9 and activin A blood levels in patients with breast cancer or prostate cancer metastatic to the bone. Anticancer Res 2007;27:1519–25.
33. Leto G, Incorvaia L, Flandina C, Ancona C, Fulfaro F, Crescimanno M, et al. Clinical impact of cystatin C/cathepsin L and follistatin/activin A systems in breast cancer progression: a preliminary report. Cancer Invest 2016;34:415–23.
34. Ogawa K, Funaba M, Tsujimoto M. A dual role of activin A in regulating immunoglobulin production of B cells. J Leukoc Biol 2008;83:1451–8.
35. Kalli M, Mpekris F, Wong CK, Panagi M, Ozturk S, Thiagalingam S, et al. Activin A signaling regulates IL13Ralpha2 expression to promote breast cancer metastasis. Front Oncol 2019;9:32.
36. Huber S, Schramm C. Role of activin A in the induction of Foxp3+ and Foxp3- CD4+ regulatory T cells. Crit Rev Immunol 2011;31:53–60.
37. Quezada SA, Peggs KS, Curran MA, Allison JP. CTLA4 blockade and GM-CSF combination immunotherapy alters the intratumor balance of effector and regulatory T cells. J Clin Invest 2006;116:1935–45.
38. Rudqvist NP, Pilones KA, Lhuillier C, Wennerberg E, Sidhom JW, Emerson RO, et al. Radiotherapy and CTLA-4 blockade shape the TCR repertoire of tumor-infiltrating T cells. Cancer Immunol Res 2018;6:139–50.
39. Wamsley JJ, Kumar M, Allison DF, Clift SH, Holzknecht CM, Szymura SJ, et al. Activin upregulation by NF-kappaB is required to maintain mesenchymal features of cancer stem-like cells in non-small cell lung cancer. Cancer Res 2015;75:426–35.
40. Rudensky AY. Regulatory T cells and Foxp3. Immunol Rev 2011;241:260–8.
41. Neuzillet C, Tijeras-Raballand A, Cohen R, Cros J, Faivre S, Raymond E, et al. Targeting the TGFbeta pathway for cancer therapy. Pharmacol Ther 2015;147:22–31.
42. Xu Z, Wang Y, Zhang L, Huang L. Nanoparticle-delivered transforming growth factor-beta siRNA enhances vaccination against advanced melanoma by modifying tumor microenvironment. ACS Nano 2014;8:3636–45.
43. Formenti SC, Lee P, Adams S, Goldberg JD, Li X, Xie MW, et al. Focal irradiation and systemic TGFbeta blockade in metastatic breast cancer. Clin Cancer Res 2018;24:2493–504.
44. Wang X, Fischer G, Hyvonen M. Structure and activation of pro-activin A. Nat Commun 2016;7:12052.
45. Loomans HA, Andl CD. Intertwining of activin A and TGFbeta signaling: dual roles in cancer progression and cancer cell invasion. Cancers 2014;7:70–91.
46. Huber S, Stahl FR, Schrader J, Luth S, Presser K, Carambia A, et al. Activin A promotes the TGF-beta-induced conversion of CD4+CD25- T cells into Foxp3+ induced regulatory T cells. J Immunol 2009;182:4633–40.

47. Vonderheide RH, Domchek SM, Clark AS. Immunotherapy for breast cancer: what are we missing? Clin Cancer Res 2017;23:2640–6.
48. Tao JJ, Cangemi NA, Makker V, Cadoo KA, Liu JF, Rasco DW, et al. First-in-human phase I study of the activin A inhibitor, STM 434, in patients with granulosa cell ovarian cancer and other advanced solid tumors. Clin Cancer Res 2019;25:5458–65.
49. Wang Z, Zhang N, Song R, Fan R, Yang L, Wu L. Activin A expression in esophageal carcinoma and its association with tumor aggressiveness and differentiation. Oncol Lett 2015;10:143–8.
50. Vanpouille-Box C, Formenti SC. Dual transforming growth factor-beta and programmed death-1 blockade: a strategy for immune-excluded tumors? Trends Immunol 2018;39:435–7.